

# Colloquium: Laboratory experiments on hydromagnetic dynamos

Agris Gailitis, Olgerts Lielausis, and Ernests Platacis

*Institute of Physics, University of Latvia, LV-2169 Salaspils 1, Latvia*

Gunter Gerbeth and Frank Stefani\*

*Forschungszentrum Rossendorf, P.O. Box 510119, D-01314 Dresden, Germany*

(Published 30 September 2002)

Cosmic magnetic fields, including the fields of planets, stars, and galaxies, are believed to be caused by dynamo action in moving electrically conducting fluids. While the theory and numerics of hydromagnetic dynamos have flourished during recent decades, an experimental validation of the effect was missing until recently. We sketch the long history towards a working laboratory dynamo. We report on the first successful experiments at the sodium facilities in Riga and Karlsruhe, and on other experiments which are carried out or planned at various places in the world.

## CONTENTS

I. The Enigmatic Field	973
II. Dynamo Basics	974
A. Cosmic magnetism	974
B. Getting started: the disk dynamo	974
C. Some mathematics	975
D. Some distinctions	976
III. Towards Laboratory Dynamos	977
A. From theory to experiment	977
B. The past attempts	977
1. Swirling sodium: Lehnert's experiment	977
2. Rotating cylinders: Lowes and Wilkinson	978
3. The " $\alpha$ -box"	978
4. Precession: another possibility for dynamo action	978
5. Fast breeders	978
IV. Present Experiments	979
A. The dynamo experiments in Riga	979
1. Basics: a single helical stream	979
2. Close to the edge: the experiment of 1987	979
3. Restart: design and preparation	979
4. The kinematic and the saturated regime	980
5. Summarizing the main results	981
B. The dynamo experiments in Karlsruhe	982
1. Multivortex flows	982
2. Mean-field model of the Karlsruhe dynamo	982
3. The experiment	983
C. Taking stock	984
V. Further and Future Experiments	984
A. Maryland	984
B. Cadarache	985
C. Madison	985
D. Grenoble	985
E. Perm	986
F. New Mexico	987
VI. Conclusions	987
Acknowledgments	987
References	988

## I. THE ENIGMATIC FIELD

"And even Thales seems, from what is recorded of him, to have supposed that the soul is something pro-

ductive of movement, if he really said that the magnet has a soul because it produces movement in iron." This sentence, found in Aristotle's "On the soul" (Aristotle, 1986), testifies that magnetism was already known around 600 B.C.

Throughout the centuries, people have been attracted by the properties of lodestone. Usually, the Chinese are said to have built the first compass in the form of a lodestone spoon, probably in the first century B.C. (cf. Needham, 1962). However, a purposefully shaped hematite bar found close to Veracruz, Mexico, suggests that the Olmec may have discovered and used the compass even earlier than 1000 B.C. (cf. Carlson, 1975).

The poles of lodestone and their attracting and repelling forces were the topic of Petrus Peregrinus's "Epistula de magnete" (Petrus Peregrinus, 1995), written in 1267, a fascinating treatise that possibly can be called the first scientific "paper" in a modern sense. Gilbert (1600), inspired by Peregrinus's work, made his own experiments with small spheres of lodestone ("terrellae"), and concluded ". . . that the terrestrial globe is magnetic and is a loadstone."

Soon after Gilbert's death, the westward drift of the Earth's magnetic field was observed by Gellibrand (1635). That unsettling discovery raised the question how such a large lodestone as Earth could undergo such a change. Halley (1692) still tried to explain the secular variation by assuming a shell structure within the Earth's interior, each sphere being independently magnetized, and each rotating slowly with respect to the others. However, the evidence against the lodestone hypothesis continued to grow. Nowadays we know that magnetite, the basic mineral of lodestone, loses its ferrimagnetism at approximately 580 °C, a temperature that is exceeded by the temperature in the Earth below a depth of about 30 km. And we know that not only planets but also stars and whole galaxies produce magnetic fields.

The laboratory experiments that are the subject of the present paper are not copies of specific cosmic bodies. Rather they are intended to underpin our *basic ideas* of cosmic magnetic-field generation, according to modern *hydromagnetic dynamo theory*.

\*Electronic address: F.Stefani@fz-rossendorf.de

## II. DYNAMO BASICS

Usually, the construction of technical devices requires a certain understanding of natural phenomena. Sometimes, however, it happens that natural phenomena are explained in terms of well-known technical processes. In the middle of the 19th century, Jedlik (cf. Simonyi, 1990), Siemens (1867), and Wheatstone (1867) had invented the technical version of the self-exciting dynamo. Only half a century later, trying to understand the magnetic field in sunspots, Larmor (1919) speculated that it might be “. . . possible for the internal cyclic motion to act after the manner of the cycle of a self-exciting dynamo, and maintain a permanent magnetic field from insignificant beginnings, at the expense of some of the energy of the internal circulation.” Larmor’s one-page communication has turned out to be the birth of the modern theory of cosmic magnetic fields.

### A. Cosmic magnetism

Magnetic fields are ubiquitous in the cosmos. They seem to exist wherever sufficiently large quantities of electrically conducting fluids can be found in convective motion mixed with rotation.

The dynamo of the Earth produces a magnetic field that is basically a dipole field with an axis slightly tilted from the geographic axis. The field intensity on the Earth’s surface is typically on the order of  $5 \times 10^{-5}$  T. Of particular interest is the observation that the Earth’s magnetic field is changing on various time scales. Most remarkable are the field reversals and the fact that their sequence shows no periodicity but seems to be completely irregular.

Besides the Earth, other planets in the solar system have magnetic fields produced by dynamo action (Merrill *et al.*, 1998). Fields are produced inside Jupiter, Saturn, Uranus, and Neptune. Possibly, a dynamo had worked inside Mars in the ancient past (Connerney *et al.*, 2001). The Mariner 10 mission in 1974–1975 had revealed the magnetic field of Mercury (Ness *et al.*, 1975), and there remain many puzzles as to how it can be produced (Southwood, 1997). The detection of the magnetic field of Ganymede, the largest Jupiter moon, was one of the major discoveries of NASA’s Galileo spacecraft mission in 1996 (Kivelson *et al.*, 1996).

The magnetic fields of sunspots were discovered by Hale (1908) at Mt. Wilson observatory, thus proving evidence that the magnetism is not a phenomenon restricted to the Earth. Accepting the tight relation of sunspots and magnetic fields, sunspot observation turns into a perfect test field for any theory of solar magnetism. What has to be explained is, first of all, the 11-year periodicity of sunspots, their migration towards the equator (the “butterfly diagram”), and the occurrence of grand minima which are superimposed upon the main periodicity (Rüdiger and Arlt, 1999).

Our Sun is not the only star with a magnetic field. Ap (A-type peculiar) stars have remarkable magnetic field strengths on the order of 1 T. The observed magnetic

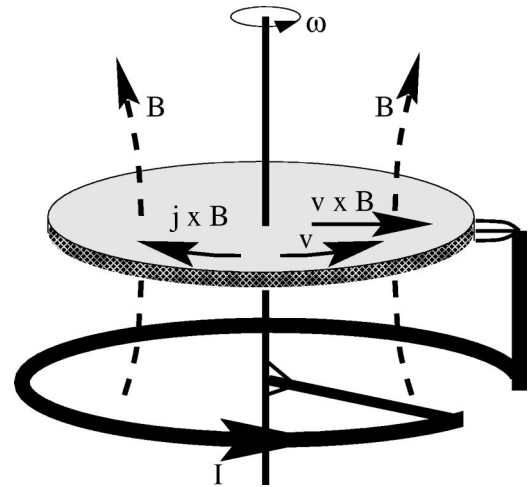


FIG. 1. The homopolar disk dynamo. A metallic disk rotates with an angular velocity  $\omega$  in a magnetic field  $\mathbf{B}$ . The emf  $\mathbf{v} \times \mathbf{B}$  points from the axis to the rim of the disk and drives a current  $I$  through the wire. The orientation of the wire is such that the external magnetic field is amplified. At a critical value of  $\omega$ , the amplification becomes infinite: self-excitation sets in. With growing magnetic field, the Lorentz force  $\mathbf{j} \times \mathbf{B}$  acts against the driving torque.

field strengths of some white dwarfs exceed 100 T, and those of some anomalous x-ray emitting pulsars reach values of  $10^{11}$  T (Kouveliotou *et al.*, 1998).

Large scale magnetic fields of the order of  $10^{-9}$  T are observed in many spiral galaxies (Beck *et al.*, 1996). Usually there is a close correlation of the magnetic field structure with the optical spiral pattern that indicates the relevance of dynamo action. It should be noted, however, that the origin of the galactic and intergalactic magnetic fields is still a matter of controversy, and that particle-physics-inspired models of magnetic field generation in the early universe are discussed as well (Grasso and Rubinstein, 2001).

### B. Getting started: the disk dynamo

Before entering the sophisticated matter of homogeneous dynamos, we discuss the very process of magnetic field self-excitation for a simple theoretical model. Basically, the homopolar disk dynamo (Fig. 1) consists of a rotating metal disk which is slidingly connected to a wire wound around the rotation axis of the disk (Bullard, 1955). Assuming that the disk rotates with an angular velocity  $\omega$  and that it is penetrated by an external magnetic field  $\mathbf{B}$ , an electromotive force (emf)  $\mathbf{v} \times \mathbf{B}$  is induced along the radial direction, with the local velocity given by  $\mathbf{v} = \omega \times \mathbf{r}$ . This emf drives a current  $I$  through the wire that amplifies the externally applied magnetic field, in the case that the rotation direction is the same as the winding direction of the wire (starting from the rim, cf. Fig. 1). The inverse amplification of the magnetic field as a function of the rotation rate is shown in Fig. 2.

Neglecting the external magnetic field, standard circuit analysis gives the relation  $L_0 I + RI = L \omega I / 2\pi$  for

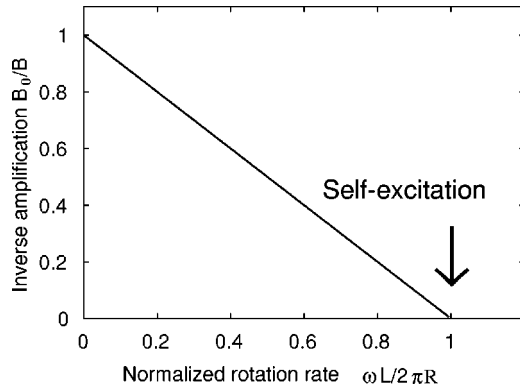


FIG. 2. Inverse amplification of the applied magnetic field in the disk dynamo. At a critical angular velocity, the amplification becomes infinite and self-excitation starts.

the current  $I$ , with  $R$ ,  $L_0$ , and  $L$  denoting the Ohmic resistance of the circuit, the self-inductance of the circuit, and the mutual inductance between the coil and a hypothetical circuit which corresponds to the rim of the disk, respectively. Evidently, this setup can work as a self-excited dynamo if the angular velocity  $\omega$  of the disk exceeds the critical value  $\omega_c = 2\pi R/L$ . Beyond that critical rotation rate the magnetic field will start to increase exponentially. This is the kinematic regime of the dynamo. With increasing magnetic field  $\mathbf{B}$  and current density  $\mathbf{j}$ , a saturation regime will be reached when the Lorentz force  $\mathbf{j} \times \mathbf{B}$  exerts a braking torque on the disk that is in equilibrium with the supposed mechanical driving torque.

Although this device looks very simple, one should notice the presence of insulating spacings between the conducting parts forcing the current in the desired direction. In contrast to multiply connected and asymmetric technical dynamos of this sort, cosmic dynamos work in singly connected electrically conducting fluids.

### C. Some mathematics

The mathematics of hydromagnetic dynamos is a fascinating topic in itself. For the theoretically inclined reader we mention, without any claim to completeness, the explanation of the dynamo effect in terms of spontaneous symmetry breaking in a field-theoretical model of magnetohydrodynamic (MHD) turbulence (Adzhemyan *et al.*, 1999), the relevance of topological methods and knot theory (Arnold and Khesin, 1998; Faddeev and Niemi, 2000), and the claimed relation of MHD with string theory (Olesen, 1996).

In the context of laboratory experiments it might suffice to derive the induction equation from textbook electromagnetism and to impart to the reader a certain feeling for how self-excitation manifests itself in a homogeneous fluid.

The equations to start with are Ampère's law, Faraday's law, and Ohm's law:

$$\nabla \times \mathbf{B} = \mu_0 \mathbf{j}, \quad (1)$$

$$\nabla \times \mathbf{E} = -\dot{\mathbf{B}}, \quad (2)$$

$$\mathbf{j} = \sigma(\mathbf{E} + \mathbf{v} \times \mathbf{B}). \quad (3)$$

The conductivity of the fluid is denoted by  $\sigma$ , and the permeability of the vacuum by  $\mu_0$  (we suppose all materials to be nonmagnetic). Note that we have skipped the displacement current in Eq. (1) as it is not relevant here. Taking the *curl* of Eqs. (1) and (3), and inserting Eq. (2), one readily arrives at the *induction equation* for the magnetic field:

$$\frac{\partial \mathbf{B}}{\partial t} = \nabla \times (\mathbf{v} \times \mathbf{B}) + \frac{1}{\mu_0 \sigma} \Delta \mathbf{B}. \quad (4)$$

In deriving Eq. (4) we have assumed, for simplicity,  $\sigma$  to be constant in the considered region, and we have exploited the fact that the magnetic field is source free:

$$\nabla \cdot \mathbf{B} = 0. \quad (5)$$

Assuming that there are no external excitations of the magnetic field from outside the considered finite region, the boundary condition for the magnetic field reads

$$\mathbf{B} = \mathbf{O}(r^{-3}) \quad \text{as } r \rightarrow \infty. \quad (6)$$

It is worthwhile to note that Eq. (4) describes the evolution of the magnetic field alone, without considering the electric field. Actually, the dominance of the magnetic field is a consequence of the quasistationarity in good conductors. The energy of the electric field is by a factor  $v^2/c^2$  smaller than the energy of the magnetic field.

The evolution of the magnetic field in Eq. (4) is governed by the competition between the diffusion and the advection of the field. For vanishing velocity the magnetic field will disappear within a typical decay time  $t_d = \mu_0 \sigma l^2$ , with  $l$  being a typical length scale of the system. On the other hand, the advection can lead to an increase of  $\mathbf{B}$  within a kinematic time  $t_k = l/v$ . If the kinematic time becomes smaller than the diffusion time, the net effect of the evolution can become positive, and hence the field will grow. Comparing the diffusion time scale with the kinematic time scale we get a dimensionless number that governs the "fate" of the magnetic field. This number is called the magnetic Reynolds number  $R_m$ :

$$R_m = \mu_0 \sigma l v. \quad (7)$$

Depending on the flow pattern, the values of the critical  $R_m$  are in the range of  $10^1 - 10^3$ .

The competition between field dissipation and production can also be understood in terms of the energy balance. Taking the scalar product of the induction equation with  $\mathbf{B}/\mu_0$ , and performing a partial integration, we find for the time evolution of the magnetic energy

$$\frac{d}{dt} \int \frac{\mathbf{B}^2}{2\mu_0} dV = - \int \mathbf{v} \cdot (\mathbf{j} \times \mathbf{B}) dV - \int \frac{\mathbf{j}^2}{\sigma} dV. \quad (8)$$

In this form, the dynamo action can be interpreted in a familiar way: the time derivative of the magnetic field

energy equals the difference between the work done (per time) by the Lorentz forces and the Ohmic losses. The Lorentz force converts kinetic energy into magnetic energy, the Ohmic dissipation converts magnetic energy into heat.

Besides the usual differential equation formulation [Eqs. (4) and (5)], dynamo action can also be made intelligible in the framework of integral equations. In the simplest case of a time-independent dynamo which is acting in an infinite region of homogeneous conductivity we can easily apply Biot-Savart's law to get

$$\mathbf{B}(\mathbf{r}) = \frac{\mu_0 \sigma}{4\pi} \int \frac{\nabla \times [\mathbf{v}(\mathbf{r}') \times \mathbf{B}(\mathbf{r}')] }{|\mathbf{r} - \mathbf{r}'|} dV'. \quad (9)$$

The source of the magnetic field is the current  $\sigma(\mathbf{v} \times \mathbf{B})$  under the integral on the right-hand side of Eq. (9). For Eq. (9) to have nontrivial solutions,  $\mathbf{B} \neq \mathbf{0}$ , the velocity field  $\mathbf{v}$  must be chosen appropriately. In particular, if we assume a certain spatial structure of  $\mathbf{v}$ , Eq. (9) turns into an eigenvalue equation for the intensity of this velocity field. For interesting numerical implementations of the integral equation method, see Gailitis (1970, 1973) and Dobler and Rädler (1998). The generalization to time-dependent dynamos was considered by Dobler and Rädler (1998), and the inclusion of boundaries was discussed by Stefani *et al.* (2000).

Finally, it is important to avoid the impression that *any* sufficiently vigorous flow will result in dynamo action. Starting with Cowling's theorem, stating that no fluid flow can maintain a purely axisymmetric magnetic field (Cowling, 1934), there are a number of anti-dynamo theorems excluding too simple structures of the velocity field or the self-excited magnetic field (cf. Fearn *et al.*, 1988; Roberts, 1994).

#### D. Some distinctions

Let us draw a few distinctions which are most relevant to characterize dynamos.

The first distinction, between *kinematic* and *dynamically consistent* dynamos, concerns the assumptions on the velocity field. If we assume the velocity to be steady, the time dependence of  $\mathbf{B}$  in Eq. (4) becomes an exponential one according to  $\mathbf{B}(\mathbf{r}, t) = \exp(\lambda t) \hat{\mathbf{B}}(\mathbf{r})$ , and the dynamo problem can be rewritten as a time-independent eigenvalue equation. In general, the eigenvalue  $\lambda$  can be complex, with a growth rate  $p$  and a frequency  $f$ :  $\lambda = p + 2\pi if$ . A velocity field  $\mathbf{v}$  is then said to work as a dynamo if  $p \geq 0$ . As in the disk dynamo case, the field then starts to grow exponentially. As we have seen, dynamo action is based on the conversion of kinetic energy into magnetic energy. It is obvious that the source of dynamo action, the velocity field, cannot stay unaffected when the magnetic field grows. Indeed, with increasing magnetic field there is an increasing Lorentz force  $\mathbf{j} \times \mathbf{B}$  acting back on the velocity field, again as in the case of the disk dynamo. In general, the evolution of the velocity field is governed by the Navier-Stokes equation,

$$\frac{\partial \mathbf{v}}{\partial t} + (\mathbf{v} \cdot \nabla) \mathbf{v} = -\frac{\nabla p}{\rho} + \frac{1}{\mu_0 \rho} (\nabla \times \mathbf{B}) \times \mathbf{B} + \nu \Delta \mathbf{v} + \mathbf{f}_d, \quad (10)$$

where  $\rho$  and  $\nu$  denote the density and the kinematic viscosity of the fluid,  $p$  is the pressure, and  $\mathbf{f}_d$  symbolizes driving forces which we leave unspecified at the moment. The Lorentz force in Eq. (10) puts Lenz's rule into action: the magnetic field acts back on the flow, in general weakening the source of its own generation. The treatment of the coupled system of Eqs. (4) and (10), that is the dynamically consistent dynamo problem, is much more intriguing than the treatment of the linear induction equation alone.

A second distinction concerns whether or not the turbulent character of practically all dynamo related flows is treated by the dynamo model. Note that in dimensionless form both Eqs. (4) and (10) are equations with small coefficients at the highest derivative. These small coefficients are  $R_m^{-1}$  for Eq. (4) and  $Re^{-1}$  for Eq. (10), where  $Re$  denotes the hydrodynamic Reynolds number  $Re = lv/\nu$ . The magnetic Prandtl number  $P_m := R_m/Re = \mu_0 \sigma \nu$  for liquid metals is of the order  $10^{-5}$ , hence  $Re$  for liquid metal dynamos is larger than  $10^6$ . Those flows are in general turbulent, the question is only about the turbulence level and its role in the dynamo process. Commonly, one distinguishes between so-called *laminar* and *mean-field* dynamo models. Laminar models are described by the unchanged Eq. (4) with neglected turbulence. The self-excited magnetic field varies on the same length scale as the velocity field does. Mean-field dynamo models, on the other hand, are relevant for highly turbulent flows. In this case the velocity and the magnetic field are considered as superpositions of mean and fluctuating parts,  $\mathbf{v} = \bar{\mathbf{v}} + \mathbf{v}'$  and  $\mathbf{B} = \bar{\mathbf{B}} + \mathbf{B}'$ . From Eq. (4) we get the equation for the mean part  $\bar{\mathbf{B}}$ ,

$$\frac{\partial \bar{\mathbf{B}}}{\partial t} = \nabla \times (\bar{\mathbf{v}} \times \bar{\mathbf{B}} + \mathcal{E}) + \frac{1}{\mu_0 \sigma} \Delta \bar{\mathbf{B}}. \quad (11)$$

Obviously, the equation for the mean field is identical to the equation for the original field, except for one additional term,

$$\mathcal{E} = \overline{\mathbf{v}' \times \mathbf{B}'}, \quad (12)$$

that represents the mean electromagnetic force due to the fluctuations of the velocity and the magnetic field. The elaboration of mean-field dynamo models in the 1960s by Steenbeck, Krause, and Rädler (1966) was a breakthrough in dynamo theory (cf. also Krause and Rädler, 1980). They had shown that the mean electromotive force in a nonmirrorsymmetric turbulence can be of the form

$$\mathcal{E} = \alpha \bar{\mathbf{B}} - \beta \nabla \times \bar{\mathbf{B}}, \quad (13)$$

with a parameter  $\alpha$  that is nonzero for helical turbulence and a parameter  $\beta$  that describes the enhancement of the electrical resistivity due to turbulence. The effect that helical fluid motion can induce an emf that is *parallel* to the magnetic field is now commonly known as the

$\alpha$ -effect. Dynamo models based on the  $\alpha$ -effect have played an enormous role in the study of solar and galactic magnetic fields, and we will later explain the physics of the Karlsruhe experiment in terms of a mean-field model with the  $\alpha$ -effect.

Third, it is useful to distinguish between *weak-field* and *strong-field dynamos*. The precise distinctive feature between both types is controversial (ratio of magnetic to kinetic energy, interaction parameter, etc.). Here we adopt the definition of Zhang and Schubert (2000) that “in a strong-field dynamo the structure and scale of the flow are sensitive to variations in the generated magnetic field,” whereas in a weak-field dynamo “the dynamic effect of the generated magnetic field can be treated as a perturbation.”

Connected with this, and in particular relevant to laboratory dynamos, there is a distinction between *constrained flow* dynamos and *free flow* dynamos. The present laboratory dynamos comprise mechanical installations to drive and guide the flow (propellers, guiding vanes, and blades). Obviously, the fewer installations present in the fluid, the more freedom the flow has to be modified and reorganized by the Lorentz forces. The idea behind free flow dynamos is to make the flow field as unconstrained as possible allowing a free evolution of the nonlinearities in the coupled Eqs. (4) and (10). It would be most interesting to drive the flow purely by convection, as in the Earth’s outer core. However, it seems to be impossible to reach velocities sufficient for dynamo action in a purely convective way in laboratory experiments, as discussed, e.g., by Tilgner (2000). Hence all present laboratory experiments have to find a compromise between a mechanical forcing of the flow and the degree of freedom of the flow for the magnetic field back reaction.

For completeness, we should also mention the distinction between *slow* and *fast* dynamos (Childress and Gilbert, 1995) which is, however, not particularly relevant for experimental dynamos.

### III. TOWARDS LABORATORY DYNAMOS

#### A. From theory to experiment

During recent decades tremendous progress has been made in the analytical understanding and the numerical treatment of hydromagnetic dynamos, which has been reported in dozens of monographs and review articles (to quote a few: Busse, 1978, 2000, 2002; Moffatt, 1978; Krause and Rädler, 1980; Inglis, 1981; Roberts and Jensen, 1992; Roberts and Soward, 1992; Childress and Gilbert, 1995; Hollerbach, 1996; Fearn, 1998; Merrill *et al.*, 1998; Roberts and Glatzmaier, 2000). Recent numerical simulations (Glatzmaier and Roberts, 1995; Kuang and Bloxham, 1997; Busse *et al.*, 1998; Christensen *et al.*, 1999; Kageyama *et al.*, 1999) share their main results with features of the Earth’s magnetic field, including the dominance of the axial dipolar component, weak nondipolar structures, and, in some cases, full polarity reversals, a behavior that is well known from pa-

leomagnetic measurements (for a recent overview, see Merrill and McFadden, 1999).

Despite those successes, a number of unsolved problems remain. The simulations of the Earth’s dynamo are carried out in parameter regions far from the real one. This concerns, in particular, the Ekman number  $E$  (the ratio of the rotation time scale to the viscous time scale) and the magnetic Prandtl number  $P_m$  (the ratio of the magnetic diffusion time to the viscous diffusion time). The Ekman number of the Earth is of the order  $10^{-15}$ , the magnetic Prandtl number is of the order  $10^{-6}$ . Present numerical simulations are carried out for values of  $E$  and  $P_m$  as small as  $E \sim 10^{-5}$  and  $P_m \sim 0.1$ . The wide gap between real and numerically tractable parameters is, of course, a continuing source of uncertainty about the physical relevance of those simulations. The usual way in fluid dynamics to deal with parameter discrepancies of this sort, namely, to apply sophisticated turbulence models, is presently hampered by the lack of reliable turbulence models for fluids that are strongly rotating and strongly interacting with a magnetic field. Here is the crucial point where laboratory experiments are unavoidable in order to collect knowledge about the turbulence structure in the (rotating or not) dynamo regime.

#### B. The past attempts

Typical values of the critical magnetic Reynolds number for different flow geometries are of the order of 100. For the best liquid metal conductor, sodium, the product of conductivity and magnetic permeability is approximately  $10 \text{ s/m}^2$ . To get an  $R_m$  of 100 the product of length and velocity has to be  $10 \text{ m}^2/\text{s}$ . It is this large value, in combination with the technical and safety problems in handling sodium, that has made the way to a working laboratory fluid dynamo so stony. To reach this value one should have more than  $1 \text{ m}^3$  sodium and use at least 100 kW of mechanical power to move it.

##### 1. Swirling sodium: Lehnert’s experiment

An early dynamo-related sodium experiment was reported by Lehnert (1958). His experiment can be considered as the prototype of a number of dynamo-related experiments which will be considered later. Lehnert had used a motor-driven disk, partly attached with radial strips, rotating in a 0.4-m-diameter vessel containing 58 l of liquid sodium. He observed the conversion of an applied poloidal magnetic field component into a toroidal field, which is an important ingredient of the dynamo process. Historically it is interesting that Lehnert did not believe in the dynamo capabilities of his device: “A fluid dynamo necessarily has to be asymmetric in order to become self-exciting. Thus it is plausible that no dynamo can exist in the configuration . . . which has a low degree of asymmetry and has been operated at angular velocities not exceeding  $47 \text{ sec}^{-1}$ .” It seems that, being well aware of the impossibility of axisymmetric magnetic field generation (Cowling, 1934), Lehnert did not fore-

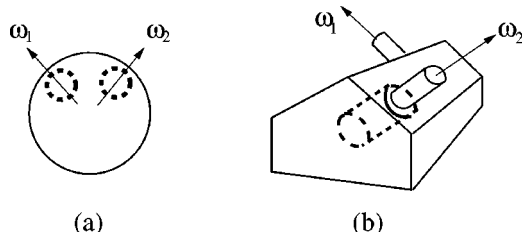


FIG. 3. Herzenberg's dynamo model. (a) Two spheres rotate around nonparallel axes. (b) The first dynamo of Lowes and Wilkinson. Two cylinders rotate in a "house-shaped" block.

see the spontaneous breaking of magnetic field symmetry allowing dynamo action for axisymmetric velocity fields as well.

## 2. Rotating cylinders: Lowes and Wilkinson

Soon after Lehnert, Lowes and Wilkinson started a long-term series of homogeneous dynamo experiments (Lowes and Wilkinson, 1963, 1968; Wilkinson, 1984). Inspired by the pioneering work of Herzenberg (1958), who had given the first rigorous existence proof for a homogeneous dynamo consisting of two rotating small spheres embedded in a large sphere, they started with the first homogeneous dynamo using two rotating cylinders in a "house-shaped" surrounding conductor (see Fig. 3). The key point for the success of this and the following experiments was the utilization of various ferromagnetic materials making the magnetic Reynolds number large, simply by a high relative magnetic permeability  $\mu_r$  (between 150 and 250).

The history of these experiments is fascinating, not only for their step-by-step improvements but also for the continuing comparison of the resulting field with geomagnetic features (Wilkinson, 1984). Starting with a simple geometry of the rotating cylinders, which produced steady and oscillating magnetic fields, the design was made more sophisticated so that it permitted the observation of field reversals. That way it was shown that a complex field structure and behavior can be produced with comparatively simple patterns of motion.

However, the experiments were flawed by the use of ferromagnetic materials (e.g., permivar, heat treated mild steel, electrical iron) and the nonlinear field behavior which is inevitably connected with these materials. One attempt to get self-excitation with rotating nonmagnetic copper cylinders failed. And, although homogeneous, all these dynamos did not allow one to study the nontrivial back reaction of the magnetic field on the fluid motion, and there was no chance to learn something about MHD turbulence.

## 3. The " $\alpha$ -box"

It was in the 1960s that the concept of mean-field dynamos and the  $\alpha$ -effect started to flourish (Steenbeck *et al.*, 1966). As said above, the essence of the  $\alpha$ -effect is that helical turbulence can produce currents *parallel* to the mean magnetic field. Compared to our book learn-

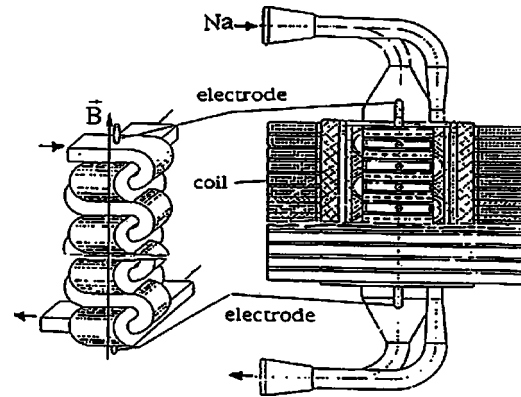


FIG. 4. The " $\alpha$ -box," the first dynamo-related experiment in Riga. The sodium flow through the helically interlaced channels produces an emf parallel to the magnetic field.

ing that currents and magnetic fields are connected via the right-hand rule, this effect is indeed remarkable.

For experimental demonstration of the  $\alpha$ -effect, Steenbeck *et al.* (1967) constructed the " $\alpha$ -box," a system of two orthogonally interlaced channels (see Fig. 4). By virtue of this special geometry, the sodium flow through this system was not mirror symmetric.

The main result of this experiment was that the induced voltage in weak fields is proportional to  $Bv^2$ , i.e., it is independent of the flow direction, and it reverses if the applied magnetic field is reversed. The  $\alpha$ -effect was therefore validated.

We only mention that recently the  $\beta$ -effect, i.e., the reduction of the electrical conductivity due to turbulence [cf. Eq. (13)], was demonstrated in an experiment by Reighard and Brown (2001).

## 4. Precession: another possibility for dynamo action

Gans (1970) has reported on an experiment which was dynamo related, too. He used a sodium-filled precessing cylinder having a 25 cm diameter and approximately the same height. The rotation rate of the cylinder could reach 3600 rpm, and the precession rate 50 rpm. Amplifications of an applied magnetic field up to a factor of 3 were observed.

In this context it should be mentioned that precession has not been completely ruled out as one possible source of planetary dynamos (Malkus, 1994). Recently, a precession-driven dynamo experiment with liquid sodium has been proposed (Léorat *et al.*, 2001).

## 5. Fast breeders

For the sake of completeness we mention a sort of dynamo investigation related to liquid metal fast breeder reactors (Bevir, 1973; Pierson, 1975; Kirko *et al.*, 1982). The magnetic Reynolds numbers in the huge pumps are indeed in the region where dynamo action may occur, and in some cases the flow topology is even helical, as is preferable for dynamo action. More recent

results indicate, however, that no dynamo action has occurred in those facilities (Plunian *et al.*, 1999; Alemany *et al.*, 2000).

#### IV. PRESENT EXPERIMENTS

For decades, a “fair” hydromagnetic dynamo experiment, i.e., an experiment with a homogeneous liquid but without ferromagnetic material, seemed to be at the edge of technical feasibility. The successful self-exciting dynamos of Lowes and Wilkinson were not *fluid* dynamos, and their results were dominated by the use of ferromagnetic materials. On the other hand, the sodium experiments of Lehnert (1958) and Steenbeck *et al.* (1967) were not intended to provide self-excitation.

At the end of 1999, two successful dynamo experiments have been carried out, one in Riga, Latvia (Gailitis *et al.*, 2000), the other in Karlsruhe, Germany (Müller and Stieglitz, 2000; Stieglitz and Müller, 2001). With a slight emphasis on the former (simply on account of our personal engagement), we report on the preparation and the results of both experiments.

##### A. The dynamo experiments in Riga

###### 1. Basics: a single helical stream

Dynamos like screw motion. Ponomarenko (1973) had investigated the “elementary cell” of dynamos: an endless helical stream moving as a solid cylinder and maintaining full electrical contact with its immobile surrounding. The solution of the induction equation for the Ponomarenko dynamo consists of a linear combination of Bessel functions within the screwing rod and within the surrounding motionless conductor. There remains a matching condition at the interface resulting in a transcendental secular equation. For large  $R_m$  Ponomarenko proved that this configuration is indeed a dynamo. The basic dynamo action in the large  $R_m$  limit has been called a “stretch-diffuse” mechanism (Gilbert, 1988; cf. also Ruzmaikin, Sokoloff, and Shukurov, 1988); it comprises the stretching of a weak radial field by the infinite helical shear across the boundary into azimuthal and axial fields aligned with the shear, as well as a restoration of the radial field by diffusion of the azimuthal field.

Gailitis and Freibergs (1976) found a critical  $R_m$  of 17.7 for the magnetic field mode with an azimuthal dependence  $\sim \exp(im\varphi)$  with  $m=1$ . This was an encouragingly low value for a magnetic instability. Unpleasantly, this instability turned out to be a *convective* one, i.e., a magnetic mode that grows exponentially in time but simultaneously moves downstream with some group velocity. In contrast to a *global* instability, a convective instability cannot be observed in a finite length system.

In other words, the problem is that magnetic field amplification takes place in the flow, but the amplified field is convected away. The key idea to overcome this dilemma was to introduce some sort of feedback. This feedback can be achieved by adding a counterflow to the central helical flow. From the latter the magnetic field will diffuse into the former which in turn transports the

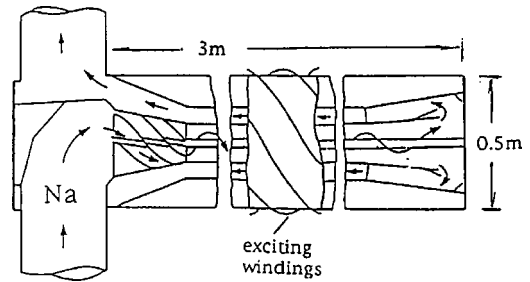


FIG. 5. The dynamo module of the 1987 experiment.

convected field back to the location of its generation. This idea was made concrete in another paper of Gailitis and Freibergs (1980). In technical terms, a *working* dynamo, i.e., a dynamo with a global instability, could consist of a helical inner flow and a surrounding backflow, connected by two flow bending regions. If we add another surrounding area with sodium at rest, which is intended to lower the critical  $R_m$  by providing suitable electrical boundary conditions, we have the central module of the Riga dynamo experiment (cf. Sec. IV.A.3 below).

###### 2. Close to the edge: the experiment of 1987

Under the guidance of two of the authors, a forerunner (see Fig. 5) of the present dynamo experiment was prepared in Riga and carried out in St. Petersburg (Gailitis *et al.*, 1987, 1989; Gailitis, 1989, 1993). Unfortunately, because of mechanical vibrations, this experiment had to be stopped before magnetic field self-excitation was reached. Nevertheless, it was possible to collect data on the essential amplification of an external seed field, which gave some indication that the value of the critical magnetic Reynolds number was in agreement with the theoretical prediction.

###### 3. Restart: design and preparation

Despite the failure to reach self-excitation, the 1987 experiment was encouraging. Since the beginnings of the 1990s, an improved version of the experiment was prepared. The main difference from the previous experiment is that the sodium flow is produced by a motor-driven propeller instead of by outer electromagnetic pumps.

Much effort has been spent to fine-tune the whole facility. The first step was to optimize the main geometric relations, in particular the relations of the three radii to each other and to the length of the system (Gailitis, 1996). The resulting shape of the central module of the dynamo is shown in Fig. 6. In a water dummy facility, a lot of tests have been carried out which were devoted to optimizing the velocity profiles (Christen *et al.*, 1998) and to ensuring the mechanical integrity of the system. All the experimental preparations were accompanied by extensive numerical simulations, using different one- and two-dimensional codes. One main result of these simulations was the optimization of the velocity profile with regard to the limited motor power resources of

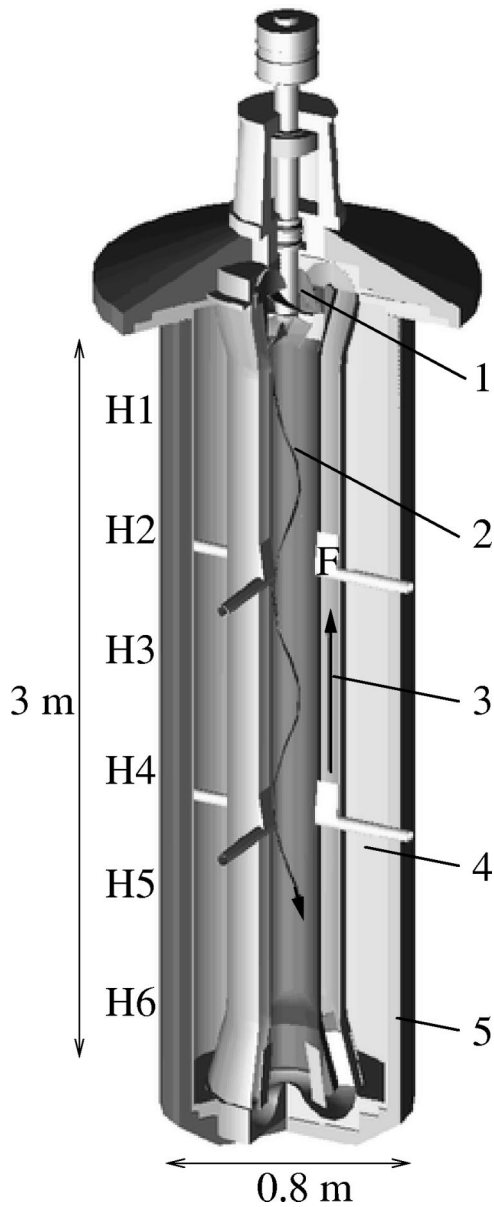


FIG. 6. The main part of the Riga dynamo facility: (1) Propeller moved via belts by two motors (not shown). (2) Helical flow region without any flowguides; flow rotation is maintained by inertia only. (3) Back-flow region. (4) Sodium at rest. (5) Thermal insulation. F: Position of the flux-gate sensor. H1–H6: Positions of six vertically aligned Hall sensors.

around 120 kW (Stefani *et al.*, 1999). Another result was the prediction of the main features of the expected magnetic field, i.e., its growth rate, frequency, and spatial structure, and the dependence of these features on the rotation rate of the propeller.

#### 4. The kinematic and the saturated regime

The first experiment at the Riga dynamo facility was carried out on 10–11 November 1999 (Gailitis *et al.*, 2000). Before the experiment could start, sodium was pumped slowly through the tubes at a temperature of 300 °C in order to ensure good electrical contact with the inner 1.5-mm stainless-steel walls. As the conductiv-

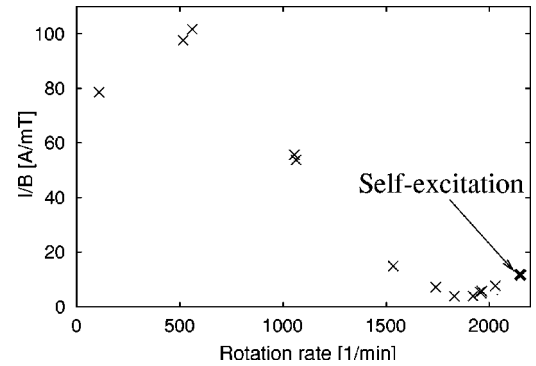


FIG. 7. Amplification of an applied magnetic field with 1 Hz. At the rightmost point (2150 rpm at 205 °C) self-excitation occurs.

ity of sodium increases with decreasing temperature, the main experiment was planned at a temperature close to 150 °C. During the cooling down period some pre-experiments were devoted to the investigation of the subcritical behavior of the dynamo. To this end, a three-phase seed-field coil was helically wound around the dynamo and fed by an ac current in order to produce a rotating magnetic field as similar as possible to the expected self-excited field. The amplification of this field, and its dependence on the propeller rotation rate, was measured by a flux-gate sensor. Figure 7 gives the inverse amplification, in terms of the relation of the applied current to the measured total field, taken at an excitation frequency of 1 Hz. In contrast to the magnetic field of the disk dynamo, the magnetic field of the Riga dynamo has a complicated spatial structure, and it rotates with a certain frequency around the dynamo axis producing an ac signal in every sensor. Nevertheless, a large part of the curve (between 500 and 1500 rpm) resembles the amplification scheme of the disk dynamo (cf. Fig. 2). This part of the curve points to an intersection with the abscissa, i.e., to infinite amplification, at about 1700 rpm. As 1 Hz is not exactly the generation frequency, the curve bends and drifts away from the abscissa above a rotation rate of 1900 rpm.

It is noteworthy that the measured signals underlying the points shown in Fig. 7 were very clean sinusoidal signals with the external frequency, with hardly any superposition of other frequencies. The observed signal shape changed suddenly at the maximum rotation rate of 2150 rpm. There, another clear-cut frequency emerged in the signal. Figure 8 shows how the measured field splits into the *amplified* external field and the *self-excited* field which was exponentially increasing in time. Hence, 11 November 1999 marked the first experimental observation of the *kinematic regime* of a hydromagnetic dynamo.

Soon after the detection of this self-excited mode, the experiment had to be stopped due to a technical problem with a seal on the propeller axis.

In July 2000, when the seal was repaired, it was possible to work at lower temperatures (down to 150 °C) and therefore at higher magnetic Reynolds numbers (Gailitis *et al.*, 2001, 2001a, 2001b; Gailitis, Lielausis,

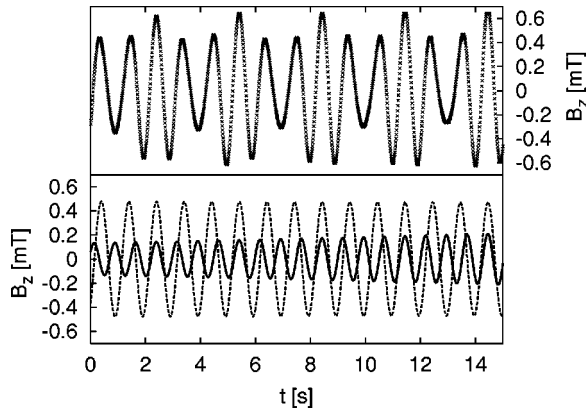


FIG. 8. Flux-gate signal measured at 2150 rpm, i.e., the right-most point in Fig. 7 (crosses). Decomposition of the signal into an amplified part with 0.995 Hz (dashed line) and a self-excited part with 1.326 Hz (full line).

Platacis, Dement'ev, *et al.*, 2002). A typical experimental run is documented in Fig. 9. The duration of this run was about 8 min. At the beginning the propeller rotation was quickly increased. Then, it was held fixed at 1950 rpm for a period of 80 sec. During this time the magnetic field grew exponentially and started to saturate. In later periods the rotation rate was slightly modified, and the dependence of the saturated field on the rotation rate was studied.

5. Summarizing the main results

From four experimental runs similar to that shown in Fig. 9, together with the runs from the November 1999 experiment, we have compiled a number of data on the

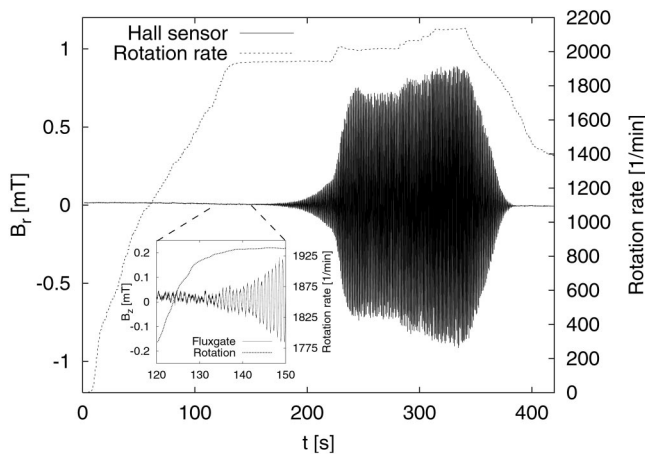


FIG. 9. One experimental run in July 2000. Rotation rate of the motors, and magnetic field measured at one Hall sensor (H4 in Fig. 6) plotted vs time. After the exponential increase of the magnetic field in the kinematic dynamo regime, the dependence of the field level on the rotation rate has been studied in the saturation regime. The temperature increased during the run from 170 to 180 °C. The inset shows the signal measured at the (inner) fluxgate sensor during the very beginning of self-excitation when the field at the (outer) Hall sensor is much below its sensitivity.

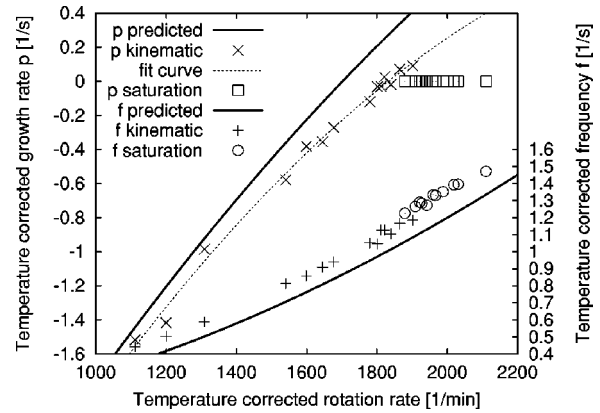


FIG. 10. Measured growth rates  $p$  and frequencies  $f$  for different rotation rates  $\Omega$  in the kinematic and the saturation regime, compared with the numerical predictions. The dotted line is a fit curve for the growth rates in the kinematic regime.  $\Omega$ ,  $p$ , and  $f$  at the temperature  $T$  were scaled to  $(\Omega_c, p_c, f_c) = \sigma(T)/\sigma(157^\circ\text{C}) [\Omega(T), p(T), f(T)]$  as required by the scaling properties of Eq. (4).

kinematic and the saturated dynamo regimes. Let us start with Fig. 10 in which the measured growth rates and frequencies are compared with our numerical predictions. For the sake of clarity all the measured data have been scaled to the sodium conductivity at a temperature of 157 °C. Starting from the left-hand side, the growth rates increase, i.e., the decay rates decrease. At the critical rotation rate of 1840 rpm, the growth rates show a sharp bend to zero, indicating that the saturation regime has been reached. (Note that there are a few positive values of the growth rates, where the magnetic fields were still small enough to belong to the kinematic regime.) The numerical prediction in the framework of kinematic dynamo theory was surprisingly good, apart from an overall shift of the measured data by about 10% towards higher rotation rates. A similar correspondence of predictions and measurements holds for the frequencies in the kinematic regime. There is a shift of about 8% towards lower rotation rates. The most surprising effect comes from the frequency data in the saturation regime. It seems that they are almost unaffected by the transition from the kinematic to the saturation regime. So what? Why does the growth rate behave as if the flow intensity were frozen to the critical one whereas the frequencies behave as if the flow intensity were completely unaffected by the back reaction?

We may come closer to the solution of this puzzle if we consider the measured magnetic field distribution along the axis of the dynamo. The data points in Fig. 11 show these distributions in the kinematic and in the saturation regime. There is a clear shift of the magnetic field towards the upper part of the dynamo.

In a first simple numerical model we have tried to understand this behavior (Gailitis, Lielausis, Platacis, Gerbeth, and Stefani, 2002). Taking into account only the azimuthal component of the Lorentz force and fitting its strength to a value that is compatible with the measured increase of the motor power in the saturation

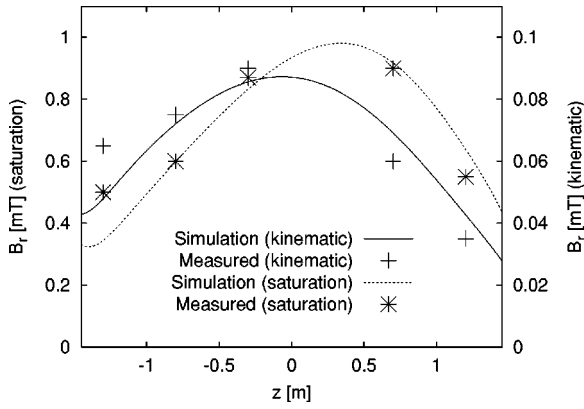


FIG. 11. Dependence of the magnetic field amplitudes on the position along the  $z$  axis of the dynamo. Measured data and predicted structure for the kinematic and the saturation regime.

regime (around 10 kW) we got the result that the reduction of the azimuthal velocity component accumulates downstream. This reduction is mirrored by the observed magnetic field distribution, depicted in the numerical curves in Fig. 11, and at the same time it explains the observed behavior of the growth rate and the frequency. To be honest, not all effects of the magnetic field in the saturation regime can be explained by our (too) simple back reaction model, but there is good hope that the back reaction can be understood by a slightly improved weak-field dynamo concept.

## B. The dynamo experiments in Karlsruhe

### 1. Multivortex flows

A dynamo experiment with a flow configuration similar to that in the present Karlsruhe experiment had been analyzed by Gailitis (1967). The underlying geophysical motivation, the basic idea, the mathematics and a final formula for the critical flow rates can already be found in that paper. The original motivation was to build a dynamo model “in which the gyrotropic turbulence is simulated by means of a certain pseudo-turbulent motion.” In other words, real helical (“gyrotropic”) turbulence was proposed to be substituted by “pseudo-turbulence,” realized by a large (but finite) number of parallel channels with a helical flow inside.

Busse (1975) considered a similar kind of dynamo. This renewed interest was triggered by theoretical and experimental studies on thermal instabilities in rapidly rotating systems (Busse, 1970, 1992; Busse and Carrigan, 1974) which had shown the appearance of convection rolls.

In 1999, self-excitation was really demonstrated in an experimental dynamo facility of this kind. Essential contributions to the prediction and the interpretation of the results of the Karlsruhe experiment have been made by Rädler *et al.* (1996, 1998) and Tilgner (1997a, 1997b).

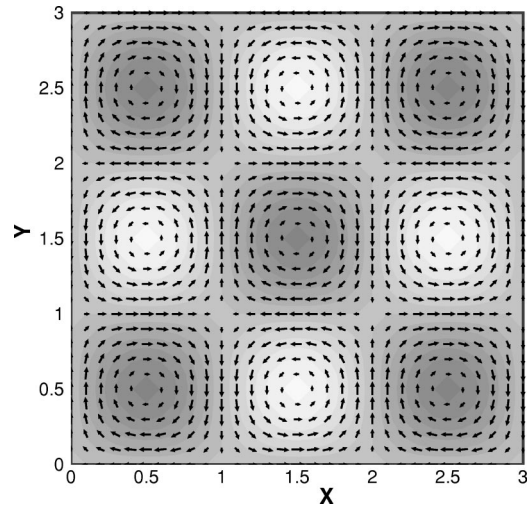


FIG. 12. Flow periodic in the  $x$  and  $y$  directions. An elementary cell of it comprises a horizontal flow (arrows) and a perpendicular flow (indicated by the gray scale).

### 2. Mean-field model of the Karlsruhe dynamo

To understand the basics of the Karlsruhe dynamo experiment, consider the velocity field in Fig. 12. It represents a flow pattern with a horizontal part and a vertical part, both are periodic in  $x$  and  $y$  directions. Roberts (1972) had shown that such a periodic flow pattern is capable of magnetic field self-excitation. For dynamos of this sort we can readily apply the mean-field machinery. We split the velocity and the magnetic field into mean fields and fluctuating fields, keeping in mind that the “fluctuations” of the velocity field are experimentally realized by the small scale, but well defined, flows in the spin generators.

It can be shown (Gailitis, 1967; Rädler *et al.*, 1998, 2002a) that for such a flow pattern without any  $z$  dependence the electromotive force acquires the form

$$\mathcal{E} = -\alpha_{\perp} [\bar{\mathbf{B}} - (\mathbf{e}_z \cdot \bar{\mathbf{B}}) \mathbf{e}_z], \tag{14}$$

i.e., an extremely anisotropic  $\alpha$ -effect that produces only electromotive forces in the  $x$  and  $y$  directions but not in the  $z$  direction.

In the specific realization of the Karlsruhe experiment the Roberts flow in each cell is replaced by a flow through two concentric channels (Fig. 13). In the central channel the flow is straight; in the outer channel it is geometrically forced on a helical path. Denoting the side length of a cell by  $a$ , the pitch of the helical channels by  $h$ , and the volumetric flow rates through the central and the helical channel by  $\dot{V}_C$  and  $\dot{V}_H$ , respectively, Rädler *et al.* (1998) gave the following expression for  $\alpha_{\perp}$ :

$$\alpha_{\perp} = \frac{\dot{V}_H}{a^2 \eta h} \left( \dot{V}_C \phi_C(\dot{V}_H / \eta h) + \frac{1}{2} \dot{V}_H \phi_H(\dot{V}_H / \eta h) \right), \tag{15}$$

where  $\eta = 1/\mu_0 \sigma$ .

The functions  $\phi_C$  and  $\phi_H$  depend, apart from the given argument  $\dot{V}_H / \eta h$ , also on the profile of the rotation. They are of the order of 1 for small values of  $\dot{V}_H$ ,

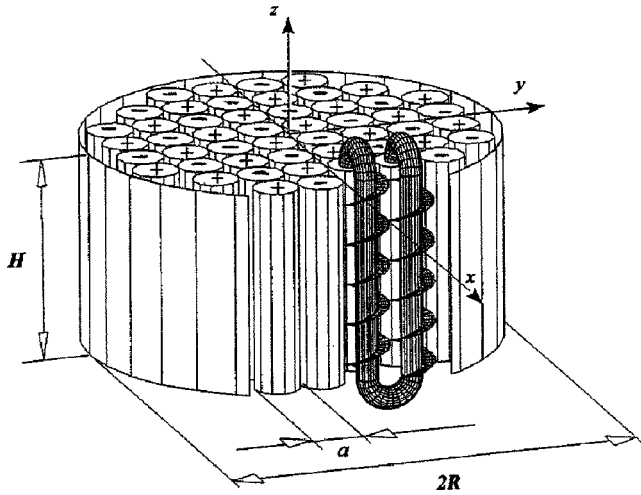


FIG. 13. Central part of the Karlsruhe dynamo facility. The module consists of 52 spin generators, each containing a central tube with nonrotating flow and an outer tube where the flow is forced on a helical path. Figure courtesy of R. Stieglitz.

but decrease to 0 for higher  $\dot{V}_H$ . The resulting nontrivial dependence of  $\alpha_\perp$  on  $\dot{V}_H$  is a consequence of the flux expulsion in rotating conductors.

For the experimentally interesting region, the isolines of the quantity  $C = \alpha_\perp R / \eta$ , which is a dimensionless measure of the  $\alpha$  effect, are plotted in Fig. 14 ( $R$  denotes the radius of the module).

Once  $\alpha_\perp$  is expressed in terms of the flow rates  $\dot{V}_C$  and  $\dot{V}_H$  one can put it into an induction equation solver in order to determine the critical value  $C^*$  of  $C$ , beyond which magnetic field self-excitation occurs. One has to be careful in order to find the critical value for the most

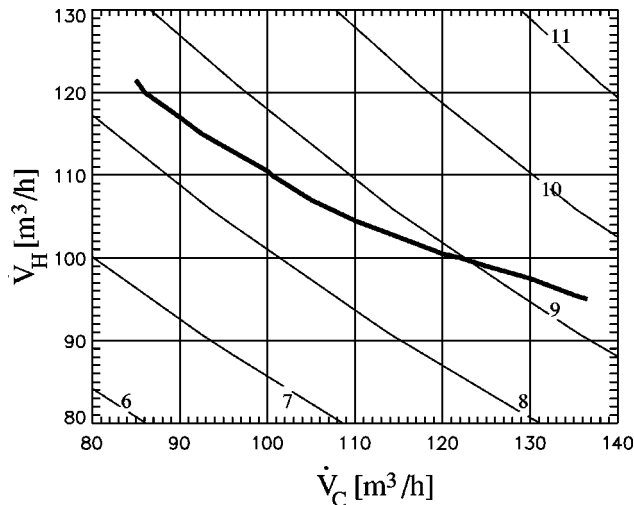


FIG. 14. Isolines of the dimensionless number  $C = \alpha_\perp R / \eta$  in the  $\dot{V}_C$ - $\dot{V}_H$  plane, resulting from Eq. (15). In a certain approximation, dynamo action should occur beyond the isoline with  $C = 8.12$  (Rädler et al., 2002a). The experimentally determined neutral line (bold), separating regions with and without dynamo action, slightly deviates from the theoretical line. Figure courtesy of K.-H. Rädler.

easily excitable modes of the magnetic field, which differ in their symmetries with respect to the axis and to the middle plane of the dynamo.

It turns out that the lowest value of  $C^*$  is achieved for a magnetic field mode with a dependence on the azimuthal angle  $\varphi$  as  $\exp(im\varphi)$  with  $m = 1$ . For this mode, Rädler et al. (2002a) gave a value of  $C^* = 8.12$ . However, this value depends on several modeling assumptions, and a shift of the experimental data towards higher values should always be expected.

Note that the mean-field approach is a natural way to treat the Karlsruhe dynamo, but not the only one. The induction equation can as well be solved for the actual velocity field (Tilgner, 1997a, 1997b). For differences between the two methods, see Tilgner and Busse (2001).

### 3. The experiment

Once the design principle of the Karlsruhe dynamo module was fixed, a fine-tuning of the geometric relations was necessary (Stieglitz and Müller, 1996). This concerned, in particular, the number of spin generators  $Z$ , the radius of the module  $R$ , the height of the module  $d$ , the difference  $\Delta r$  of the radii of the inner and the outer tube, and the pitch height  $h$ . The criterion was, naturally, to achieve the highest possible  $\alpha_\perp$  for a given pump power. One can easily imagine that a large value of  $h$  would decrease the pressure losses in the helical channel but would at the same time also decrease the value of  $\alpha_\perp$ .

The output of this optimization was the following choice of the above values:  $Z = 52$ ,  $R = 0.85$  m,  $d = 0.703$ ,  $\Delta r = 0.055$  m,  $a = 0.21$  m, and  $h = 0.19$  m.

The Karlsruhe dynamo facility includes the central dynamo module [Fig. 15(a)], three MHD pumps, a tank, a cooling device, and control and measurement units. In contrast to the Riga setup in which a single swirling flow forces the magnetic field pattern to rotate, in the Karlsruhe setup an equal number of streams with either rotation direction produce a dc field.

Figure 15 documents the experiment carried out in December 1999 (Müller and Stieglitz, 2000; Stieglitz and Müller, 2001). The scheme in Fig. 15(a) depicts the dynamo module with the 52 spin generators and defines the coordinate system for the location and direction of the Hall probes. The remaining three plots [Figs. 15(b)–(d)] show the magnetic field behavior at different positions and for different directions. The signals were recorded after the central flow rate  $\dot{V}_C$  was set to a constant value of  $115$  m<sup>3</sup>/h and the flow rate  $\dot{V}_H$  in the helical ducts was increased from  $95$  m<sup>3</sup>/h to  $107$  m<sup>3</sup>/h at a time 30 s from the start of the experiment. It is fascinating to see that the field needs about one and a half minutes to grow. Only at a time 120 s does it start to saturate at a few mT. Hence December 1999 marked the first experimental observation of the *saturated regime* of a hydromagnetic dynamo.

Meanwhile, some other experiments have been carried out at the Karlsruhe facility. One of the main results of all these experiments is a stability diagram (Fig. 14).

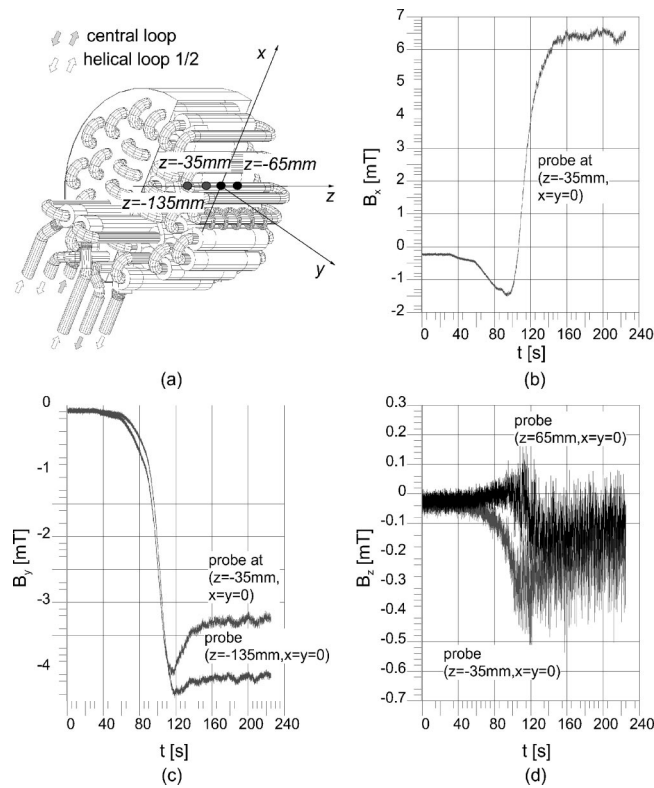


FIG. 15. Self-excitation and saturation in the Karlsruhe dynamo experiment. (a) The dynamo module with the connections between the spin generators and the supply pipes. (b)–(d) Simultaneously recorded Hall sensor signals in the inner bore of the module. Figure courtesy of R. Stieglitz.

The experimentally determined neutral line, separating dynamo and nondynamo regions, corresponds to values of  $C^*$  in the region of 8.4–9.3. Hence the numerical prediction,  $C^* = 8.12$ , resulting from mean-field theory (Rädler *et al.*, 2002a) was quite reasonable.

Work is going on in order to improve the kinematic dynamo simulations (Rädler *et al.*, 2002a; Tilgner, 2002) and to make initial attempts to understand the saturated regime (Tilgner and Busse, 2001; Rädler *et al.*, 2002b).

### C. Taking stock

What did we learn, after all, from the dynamo experiments in Riga and Karlsruhe? Killjoys could argue that (pre-)Maxwell's equations and Ohm's law have been validated once more, laws that nobody seriously doubted. As for the kinematic dynamo regime, there is indeed some rationale behind such an opinion. Given a well-known laminar velocity distribution, the numerical solution of the induction equation is in principle no longer a problem. But even for this kinematic regime there are open questions, in particular concerning the role of turbulence. The experiments have shown that dynamo action is a *robust* phenomenon, even if the velocity structure is only approximately known and the turbulence is not considered. It is also robust with respect to imperfect boundary conditions. Kinematic dy-

namo work, and rough numerical simulations are fairly appropriate to describe them. This was generally believed; now we *know* it.

Killjoys could also object that the flows in both experiments are not free enough to allow for nontrivial back reactions. This is not true. For the Riga experiment we have shown that there is room for a remarkable deformation of the flow structure. At the propeller rotation rate reached the Riga dynamo is a weak-field dynamo, understandable within the framework of a perturbation expansion around the unperturbed flow. But it is worthwhile to understand this kind of saturation experimentally and numerically before switching over to the study of strong-field dynamos.

The back reaction effects in Karlsruhe are a bit more constrained, but nevertheless they are interesting enough to warrant analysis.

## V. FURTHER AND FUTURE EXPERIMENTS

We have prominently portrayed the Riga and Karlsruhe experiments because they have shown magnetic field self-excitation. Some of the experiments that will be sketched now have been carried out even before those two. Some others are presently being carried out and it might happen that they may have already succeeded during the time this paper is in press. Some of the experiments are focusing on certain flow topologies in spheres and cylinders that had been the subject of intense numerical computations (Bullard and Gellman, 1954; Lilley, 1970; Pekeris *et al.*, 1973; Kumar and Roberts, 1975; Dudley and James, 1989; Nakajima and Kono, 1991; Holme, 1997). These topologies are classified with respect to the different numbers of poloidal and toroidal eddies. The notation  $s_2 + t_2$ , for example, stands for two poloidal eddies ( $s_2$ ) that are inward directed in the equatorial plane (indicated by the +), together with two counter-rotating toroidal eddies ( $t_2$ ).

### A. Maryland

Under the guidance of D. Lathrop at the University of Maryland, there have been impressive efforts to build a working dynamo (Peffley, Goumivski, *et al.*, 2000; Shew *et al.*, 2001).

The first experiment (Fig. 16) was motivated by common ideas about planetary convection. A 0.2-m-diameter titanium vessel containing 1.5 l of liquid sodium was heated on the outer side and cooled at the axis. The fast rotation (up to 25 000 rpm) was intended to induce centrifugally driven convection, with the centrifugal force as a substitute for gravitation in the planetary case. The second experiment (Fig. 17) consisted of a 0.3-m-diameter steel sphere. A total of 15 l of sodium was stirred by two counter-rotating propellers, each powered by 7.4-kW motors.

In neither of these two experiments was there any sign of magnetic field self-excitation. However, in the second experiment, it was possible to decrease the decay rate of an applied magnetic field by about 30% compared to the

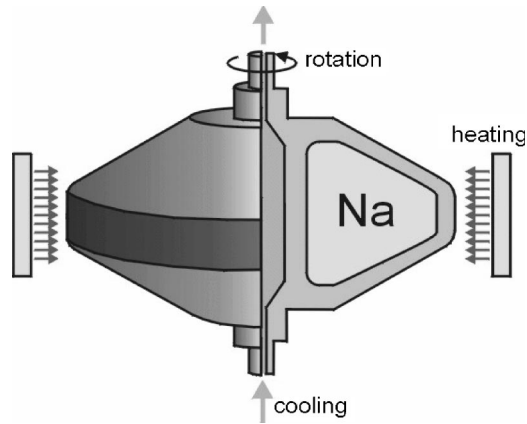


FIG. 16. The first dynamo experiment in Maryland. A rapidly rotating torus is heated at the rim and cooled at the axis. Figure courtesy of D. Lathrop.

unstirred fluid (Peffley, Cawthorne, and Lathrop, 2000). This was achieved for a magnetic Reynolds number of about 65. Further experiments with larger spheres are planned.

#### B. Cadarache

On the premises of the research center in Cadarache (France), a group guided by J.-F. Pinton has built and run a dynamo experiment under the acronym VKS. VKS means “von Kármán sodium,” and “von Kármán” stands for the flow between two rotating disks (cf. Zandbergen and Dijkstra, 1987).

The flow is produced inside a cylindrical vessel with equal diameter and height,  $2r = H = 0.4$  m [Fig. 18(a)]. The counter-rotating flows [Figs. 18(b) and (c)] are produced by disks driven by two 75-kW motors at rotation rates up to 1500 rpm. The von Kármán flow geometry has been chosen as it is the realization of the  $s2 + t2$  flow that is known to yield self-excitation at comparably low values of  $R_m$ . The disadvantage of this flow is a high sensitivity of the critical  $R_m$  on the precise relation of poloidal and toroidal velocity components. In addition, the counter-rotation at the equatorial plane is a powerful source of turbulence, making numerical predictions based on laminar flows doubtful.

The results of this experiments have been published by Marié *et al.* (2001), Bourgoïn *et al.* (2001), and Marié *et al.* (2002). Up to the present no self-excitation has been achieved, although remarkable deformations of applied magnetic fields have been measured.

#### C. Madison

Since 1997, C. B. Forest and his colleagues have prepared a dynamo project at the University of Wisconsin-Madison (O’Connell *et al.*, 2001; Forest *et al.*, 2002). Like the second experiment in Maryland, the Madison dynamo is a sphere filled with liquid sodium which is driven by two propellers. The flow topology is again the  $s2 + t2$  topology consisting of two counter-rotating toroi-

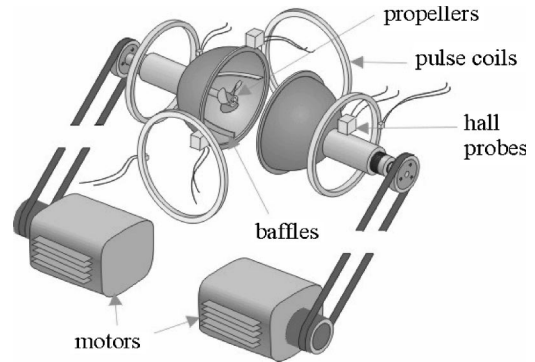


FIG. 17. The second dynamo experiment in Maryland. In a 0.3-m-diameter sphere different flows have been produced by propellers. Figure courtesy of D. Lathrop.

dal flows and two poloidal flows which are pointing inward in the equatorial plane.

A lot of effort has been spent in the numerical optimization of the precise geometry of the flow. Even then, there remained the problem of finding an adequate propeller configuration that drives the desired flow. Water pre-experiments have been carried out with a power supply of 35 kW, corresponding in sodium to an  $R_m$  of 70. The velocity profiles have been carefully measured and analyzed, leading to the result that an interpolation to an  $R_m$  of 100 should give a working dynamo. The power supply at the final sodium experiment is 150 kW which should be enough to meet the goal, provided, and here is the big uncertainty, that one takes into account only the mean velocity. The fluctuations have also been measured, giving a turbulence degree of approximately 40%. The turbulence consists not only of high-frequency fluctuations but also contains low-frequency fluctuations with a period comparable to the resistive diffusion time.

In order to estimate the effect of these low-frequency fluctuations on the growth rate of the magnetic field, the measured mean flow velocities have been varied many times, using a Monte Carlo sampling, by the measured fluctuation levels (O’Connell *et al.*, 2001). The result is a histogram of growth rates whose dependence upon the chosen stochastic profile provides hope of getting growing eigenmodes, at least for a certain fraction of time. In this respect, turbulence makes the success of the Madison experiment somehow unpredictable, but in case of success it might also give rise to an interesting behavior of the dynamo, possibly with an on-off intermittence of the magnetic field.

#### D. Grenoble

A group of geophysicists in Grenoble plans to build a laboratory dynamo as similar as possible to the Earth’s dynamo (Cardin *et al.*, 2002). Continuing the tradition of former geophysically inspired experiments (Brito *et al.*, 1995), the Grenoble ansatz relies heavily on the concept of *magnetostrophic* equilibrium between the Coriolis forces (in a rotating sphere) and the Lorentz forces.

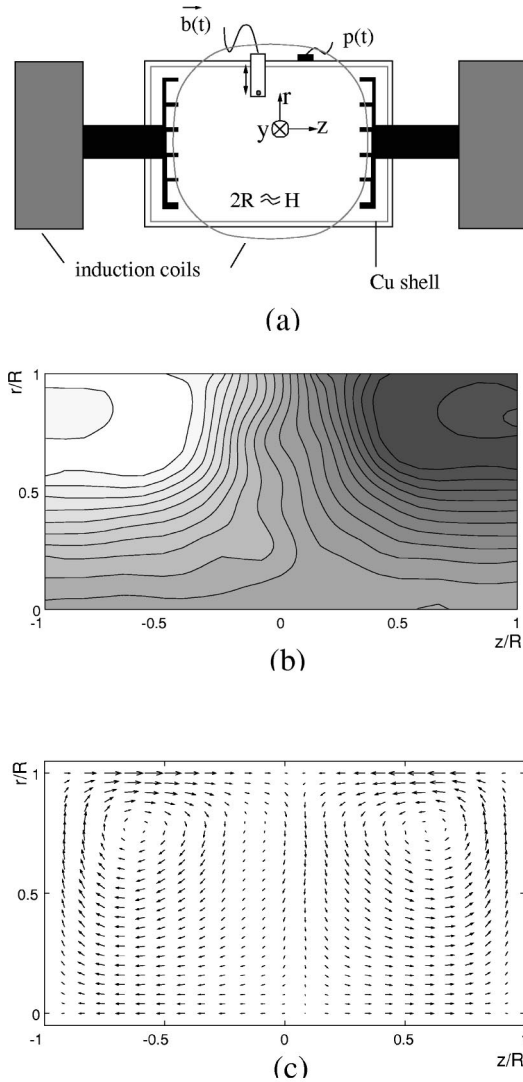


FIG. 18. The VKS experiment in Cadarache. (a) The experimental design with the disks rotating in the cylinder, the induction coils and the Hall and pressure probes. (b) Isolines of the toroidal component of the time averaged velocity for the case of counter-rotating disks. (c) Vector plot of the poloidal component of the time averaged velocity. Figure courtesy of the VKS team.

A large version of this experiment is expected to be of 1 m radius, with the outer sphere rotating at around 400 rpm, and an inner sphere of radius 0.5 m rotating at about 560 rpm. The power to drive such a dynamo is estimated to be of the order 650 kW, which is four times the power used in the Riga experiment. Presently, a small version of such an experiment, called DTS (“Derviche Tourneur Sodium”), is being prepared in Grenoble, with the special feature of a permanent magnet in the inner sphere in order to study the magneto-strophic regime even when self-excitation is expectedly not achieved.

### E. Perm

The dynamo experiments discussed so far are large scale in size and driving power. The idea of a dynamo

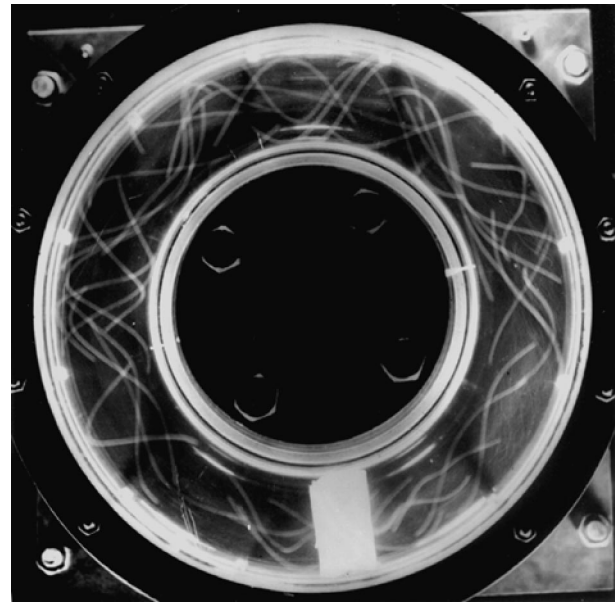


FIG. 19. Helical flow that develops after the abrupt brake of the torus in the Perm experiment, visualized by polystyrene particles. The white bar at the bottom of the picture represents the diverter. Figure courtesy of P. Frick.

with low necessary motor power has been pursued in the group of P. Frick at the Institute of Continuous Media Mechanics in Perm, Russia (Frick *et al.*, 2001, 2002). The experiment is based on the fact that a nonstationary helical flow of the Ponomarenko type can be produced within a torus when its rotation is abruptly braked and a fixed diverter forces the inertially continuing flow on a helical path. This concept is very attractive not only with respect to the low motor power that is necessary to slowly accelerate the torus, but also with respect to the fact that the sodium can be perfectly confined in the torus without any need for complicated sealing. A less attractive feature is the nonstationarity of the flow allowing only the study of a transient growth and decay of a magnetic field. A technical problem is, of course, the control of the abrupt braking action when a large amount of kinetic energy must be dissipated at once and considerable stresses and strains act on parts of the facility.

Extensive water pre-experiments and numerical simulations have been carried out to optimize and predict magnetic self-excitation in such a nonstationary dynamo. Figure 19 gives an impression of the flow that appears shortly after the brake of the torus. The major radius of the water-filled torus is 10 cm, the minor radius is 2.7 cm. The photograph was taken 1.5 s after the full stop.

Water measurements and numerical optimization have led to the proposal of a realistic sodium experiment with the following dimensions: major radius of the torus, 40 cm; minor radius of the torus, 12 cm; mass of sodium, 115 kg; rotation rate, 3000 rpm; maximal velocity, 140 m/s; effective magnetic Reynolds number, 40; minimal braking time, 0.1 s. For such a configuration it is expected that the magnetic field will grow within a time period of approximately half a second.

## F. New Mexico

A sodium experiment with a claimed direct relevance for a concrete cosmic dynamo is presently under construction at the New Mexico Institute of Mining and Technology (Colgate *et al.*, 2001, 2002). The title of the project is “The  $\alpha-\Omega$  accretion disk dynamo that powers active galactic nuclei (AGN) and creates the magnetic field of the universe.” Here, we can only touch upon the astrophysical background that has been the subject of enormous work during the last decade (for a comprehensive review see Balbus and Hawley, 1998). “Accretion” refers to the accumulation of matter onto a heavy cosmic body, under the influence of its pull of gravity. Accretion disks appear as (a) protostellar disks from which stellar systems are born, (b) disks around accreting compact stars in binary systems, and (c) disks in active galactic nuclei (AGN). For decades, it has been a major problem to understand how accretion works in reality. On the one hand, the release of gravitational energy is essential to the accretion process as well as a powerful source of the observed luminosity; on the other hand, the angular momentum has to be conserved and cannot be easily withdrawn from the infalling matter. A purely laminar shear would be totally insufficient to explain the dissipation and the necessary transport of angular momentum. Turbulence could do that job, but Rayleigh’s criterion that differentially rotating disks become unstable when the specific angular momentum,  $\Omega(r)r^2$ , increases inwards, is not fulfilled for disks which are governed mainly by Kepler’s law  $\Omega(r) = (GM/r^3)^{1/2}$ .

This puzzle has been solved by Balbus and Hawley (1991) who had shown that a magnetic field prevents gas flow in the disk from being laminar. The *magnetorotational instability* that arises makes the gas flow turbulent, thus allowing for increased heat production and angular momentum transport. What is more, the resulting turbulence is capable of maintaining a dynamo (Drecker *et al.*, 2000). In effect the kinetic energy is transformed into magnetic energy which, in turn, keeps the instability going, thereby feeding the turbulence.

Dynamo action in accretion disks is the background of the New Mexico dynamo experiment. The experiment is designed to simulate the field deformations produced by Keplerian rotation and the collision of stars with the accretion disk. As a side remark, we mention also recent investigations into the possibility of studying the magnetorotational instability in the laboratory (Ji *et al.*, 2001; Rüdiger and Zhang, 2001).

Figure 20 shows the scheme of a water pre-experiment which also illustrates the essentials of the envisioned sodium experiment. The differential rotation of the inner and outer cylinders is intended to produce a Couette flow [with  $\Omega(r) \sim r^{-2}$  instead of  $\Omega(r) \sim r^{-3/2}$  for a Keplerian flow]. In addition to the Couette flow, plumes are produced by driven pulsed jets. The planned  $R_m$ , based on the rotation alone, is 130, the corresponding  $R_m$  for the plumes is 15 (Colgate *et al.*, 2001). The water experiments have already revealed that the differ-

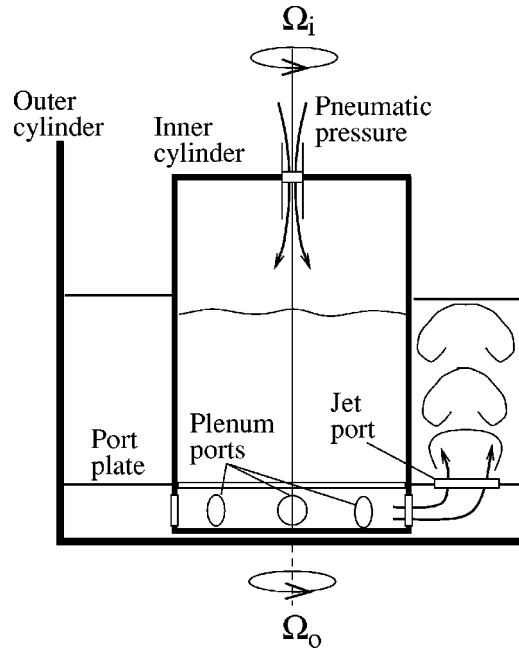


FIG. 20. Pulsed Jet Rotation Experiment, a water test facility for the New Mexico dynamo experiment. The inner and outer radii are 7.5 and 15 cm, respectively (cf. Colgate *et al.*, 2001).

ential rotation of the Couette flow speeds up the anticyclonic rotation of the plumes. This anticyclonic rotation forms the basis for the  $\alpha$ -effect of the  $\alpha-\Omega$  dynamo.

## VI. CONCLUSIONS

With the success of the complementary sodium experiments in Riga and Karlsruhe the science of homogeneous dynamos has been pushed forward. Kinematic dynamo theory has been shown to be correct and robust with respect to low levels of turbulence and complicated boundary and interface conditions. The observed saturation effects are nontrivial as they concern not only the expected increase of motor power but also the redistributions of the flow. A number of other experiments are currently being prepared or carried out, with varying theoretical backgrounds, flow topologies, and technical refinements. If these experiments work, they will open up flow regimes with higher degrees of freedom and turbulence. None of these laboratory facilities is a perfect model of a planetary, a stellar, or a galactic dynamo. But all of them will widen our knowledge of hydromagnetic dynamos in general. Hopefully, one day geophysics and astrophysics will profit from these experiments.

## ACKNOWLEDGMENTS

We thank the Latvian Science Council for support under grants 96.0276 and 01.0502, the Latvian Government and the International Science Foundation for support under joint grant LJD100, the International Science Foundation for support under grant LFD000, and the Deutsche Forschungsgemeinschaft for support under INK 18/A1-1. The interest and support of Wolf Häfele is

gratefully acknowledged. We are indebted to Karl-Heinz Rädler for many valuable comments on the manuscript. We commemorate Max Steenbeck, who initiated our work on the subject.

## REFERENCES

- Adzhemyan, L. Ts., N. V. Antonov, and A. N. Vasiliev, 1999, *The Field Theoretic Renormalization Group Theory in Fully Developed Turbulence* (Gordon and Breach, London).
- Alemanly, A., Ph. Marty, F. Plunian, and J. Soto, 2000, *J. Fluid Mech.* **403**, 262.
- Aristotle, 1986, *De anima (On the soul)* (Penguin, Harmondsworth), pp. 135–136.
- Arnold, V. I., and B. A. Khesin, 1998, *Topological Methods in Hydrodynamics* (Springer, New York).
- Balbus, S. A., and J. F. Hawley, 1991, *Astrophys. J.* **376**, 214.
- Balbus, S. A., and J. F. Hawley, 1998, *Rev. Mod. Phys.* **70**, 1.
- Beck, R., A. Brandenburg, D. Moss, A. Shukurov, and D. Sokoloff, 1996, *Annu. Rev. Astron. Astrophys.* **34**, 155.
- Bevir, M. K., 1973, *J. Br. Nucl. Energy Soc.* **12**, 455.
- Bourgoin, M., L. Marié, F. Pétrélis, C. Gasquet, A. Guigon, J.-B. Luciani, M. Moulin, F. Namer, J. Burguete, A. Chiffaudel, F. Daviaud, S. Fauve, P. Odier, and J.-F. Pinton, 2002, *Phys. Fluids* **14**, 3046.
- Brito, D., P. Cardin, H.-C. Nataf, and G. Marollet, 1995, *Phys. Earth Planet. Inter.* **91**, 77.
- Bullard, E. C., 1949, *Proc. R. Soc. London, Ser. A* **197**, 433.
- Bullard, E. C., 1955, *Proc. Cambridge Philos. Soc.* **51**, 744.
- Bullard, E. C., and H. Gellman, 1954, *Philos. Trans. R. Soc. London, Ser. A* **247**, 213.
- Busse, F. H., 1970, *J. Fluid Mech.* **44**, 441.
- Busse, F. H., 1975, *Geophys. J. R. Astron. Soc.* **42**, 437.
- Busse, F. H., 1978, *Annu. Rev. Fluid Mech.* **10**, 435.
- Busse, F. H., 1992, in *Evolution of Dynamical Structures in Complex Systems*, edited by R. Friedrich and A. Wunderlin, Springer Proceedings in Physics Vol. 69 (Springer, Berlin), pp. 197–208.
- Busse, F. H., 2000, *Annu. Rev. Fluid Mech.* **31**, 383.
- Busse, F. H., 2002, *Phys. Fluids* **14**, 1301.
- Busse, F. H., and C. R. Carrigan, 1974, *J. Fluid Mech.* **62**, 579.
- Busse, F. H., E. Grote, and A. Tilgner, 1998, *Stud. Geophys. Geod.* **42**, 1.
- Cardin, P., D. Brito, D. Jault, H.-C. Nataf, and J.-P. Masson, 2002, *Magnetohydrodynamics* **38**, 177.
- Carlson, J. B., 1975, *Science* **189**, 753.
- Childress, S., and A. D. Gilbert, 1995, *Stretch, Twist, Fold: The Fast Dynamo* (Springer, Berlin).
- Christen, M., H. Hänel, and G. Will, 1998, in *Beiträge zu Fluidenergiemaschinen 4*, edited by W. H. Faragallah and G. Grabow (Faragallah-Verlag und Bildarchiv, Sulzbach/Ts.), pp. 111–119.
- Christensen, U., P. Olson, and G. A. Glatzmaier, 1999, *Geophys. J. Int.* **138**, 393.
- Colgate, S. A., H. Li, and V. Pariev, 2001, *Phys. Plasmas* **8**, 2425.
- Colgate, S. A., V. I. Pariev, H. F. Beckley, R. Ferrel, V. D. Romero, and J. C. Weatherall, 2002, *Magnetohydrodynamics* **38**, 129.
- Connerney, J. E. P., M. H. Acuña, P. J. Wasilewski, G. Kletetschka, N. F. Ness, H. Rème, R. P. Lin, and D. L. Mitchell, 2001, *Geophys. Res. Lett.* **28**, 4015.
- Cowling, T. G., 1934, *Mon. Not. R. Astron. Soc.* **140**, 39.
- Dobler, W., and K.-H. Rädler, 1998, *Geophys. Astrophys. Fluid Dyn.* **89**, 45.
- Drecker, A., G. Rüdiger, and R. Hollerbach, 2000, *Mon. Not. R. Astron. Soc.* **317**, 45.
- Dudley, M. L., and R. W. James, 1989, *Proc. R. Soc. London, Ser. A* **425**, 407.
- Faddeev, L., and A. J. Niemi, 2000, *Phys. Rev. Lett.* **85**, 3416.
- Fearn, D. R., 1998, *Rep. Prog. Phys.* **61**, 175.
- Fearn, D. R., P. H. Roberts, and A. M. Soward, 1988, in *Energy, Stability, and Convection*, edited by G. P. Galdi and B. Straughan (Longmans, New York), pp. 60–324.
- Forest, C. B., R. A. Bayliss, R. D. Kendrick, M. D. Nornberg, R. O'Connell, and E. J. Spence, 2002, *Magnetohydrodynamics* **38**, 107.
- Frick, P., S. Denisov, S. Khripchenko, V. Noskov, D. Sokoloff, and R. Stepanov, 2001, in *Dynamo and Dynamics, a Mathematical Challenge*, edited by P. Chossat, D. Armbruster, and I. Oprea (Kluwer, Dordrecht), pp. 1–8.
- Frick, P., V. Noskov, S. Denisov, S. Khripchenko, D. Sokoloff, R. Stepanov, and A. Sukhanovsky, 2002, *Magnetohydrodynamics* **38**, 143.
- Gailitis, A., 1967, *Magnetohydrodynamics (N.Y.)* **3**, 23.
- Gailitis, A., 1970, *Magnetohydrodynamics (N.Y.)* **6**, 14.
- Gailitis, A., 1973, *Magnetohydrodynamics (N.Y.)* **9**, 445.
- Gailitis, A., 1989, in *Topological Fluid Mechanics*, Proceedings of the IUTAM Symposium, edited by H. K. Moffatt and A. Tsinober (Cambridge University, Cambridge, England), pp. 147–156.
- Gailitis, A., 1993, in *Solar and Planetary Dynamos*, edited by M. R. E. Proctor, P. C. Matthews, and A. M. Rucklidge (Cambridge University, Cambridge, UK), pp. 91–98.
- Gailitis, A., 1996, *Magnetohydrodynamics (N.Y.)* **32**, 58.
- Gailitis, A., and Ya. Freibergs, 1976, *Magnetohydrodynamics (N.Y.)* **12**, 127.
- Gailitis, A., and Ya. Freibergs, 1980, *Magnetohydrodynamics (N.Y.)* **16**, 116.
- Gailitis, A., B. G. Karasev, I. R. Kirillov, O. A. Lielausis, S. M. Luzhanskii, A. P. Ogorodnikov, and G. V. Preslitskii, 1987, *Magnetohydrodynamics (N.Y.)* **23**, 349.
- Gailitis, A., B. G. Karasev, I. R. Kirillov, O. A. Lielausis, and A. P. Ogorodnikov, 1989, in *Liquid Metal Magnetohydrodynamics*, edited by J. Lielpeteris and R. Moreau (Kluwer, Dordrecht), pp. 413–419.
- Gailitis, A., O. Lielausis, S. Dement'ev, E. Platacis, A. Ciferons, G. Gerbeth, Th. Gundrum, F. Stefani, M. Christen, H. Hänel, and G. Will, 2000, *Phys. Rev. Lett.* **84**, 4365.
- Gailitis, A., O. Lielausis, E. Platacis, S. Dement'ev, A. Ciferons, G. Gerbeth, Th. Gundrum, F. Stefani, M. Christen, and G. Will, 2001, *Phys. Rev. Lett.* **86**, 3024.
- Gailitis, A., O. Lielausis, E. Platacis, S. Dement'ev, A. Ciferons, G. Gerbeth, Th. Gundrum, F. Stefani, M. Christen, and G. Will, 2002, *Magnetohydrodynamics* **38**, 5.
- Gailitis, A., O. Lielausis, E. Platacis, G. Gerbeth, and F. Stefani, 2001a, *Magnetohydrodynamics* **37**, 71.
- Gailitis, A., O. Lielausis, E. Platacis, G. Gerbeth, and F. Stefani, 2001b, in *Dynamo and Dynamics, a Mathematical Challenge*, edited by P. Chossat, D. Armbruster, and I. Oprea (Kluwer, Dordrecht), pp. 9–16.
- Gailitis, A., O. Lielausis, E. Platacis, G. Gerbeth, and F. Stefani, 2002, *Magnetohydrodynamics* **38**, 15.
- Gans, R. F., 1970, *J. Fluid Mech.* **45**, 111.

- Gellibrand, H., 1635, *A Discourse Mathematical on the Variation of the Magnetical Needle*, reprint edited by G. Hellmann (A. Asher, Berlin, 1887).
- Gilbert, A. D., 1988, *Geophys. Astrophys. Fluid Dyn.* **44**, 241.
- Gilbert, W., 1600, *De Magnete*, translated by P. F. Mottelay (Dover, New York, 1958).
- Glatzmaier, G. A., and P. H. Roberts, 1995, *Nature (London)* **377**, 203.
- Grasso, D., and H. R. Rubinstein, 2001, *Phys. Rep.* **348**, 163.
- Gubbins, D., 1974, *Rev. Geophys. Space Phys.* **12**, 137.
- Hale, G. E., 1908, *Astrophys. J.* **28**, 315.
- Halley, E., 1692, *Philos. Trans. R. Soc. London* **17**, 470.
- Herzenberg, A., 1958, *Philos. Trans. R. Soc. London, Ser. A* **250**, 543.
- Hollerbach, R., 1996, *Phys. Earth Planet. Inter.* **98**, 163.
- Holme, R., 1997, *Phys. Earth Planet. Inter.* **102**, 105.
- Inglis, D. R., 1981, *Rev. Mod. Phys.* **53**, 481.
- Ji, H., J. Goodman, and A. Kageyama, 2001, *Mon. Not. R. Astron. Soc.* **325**, L1.
- Kageyama, A., M. M. Ochi, and T. Sato, 1999, *Phys. Rev. Lett.* **82**, 5409.
- Kirko, I. M., G. E. Kirko, A. G. Sheinkman, and M. T. Teli-chko, 1982, *Dokl. Akad. Nauk SSSR* **266**, 854.
- Kivelson, M. G., K. K. Khurana, C. T. Russell, R. J. Walker, J. Warnecke, F. V. Coroniti, C. Polanskey, D. J. Southwood, and G. Schubert, 1996, *Nature (London)* **384**, 537.
- Kouveliotou, C., S. Dieters, T. Strohmayer, J. van Paradijs, G. J. Fishman, C. A. Meegan, K. Hurley, J. Kommers, I. Smith, D. Frail, and T. Murakami, 1998, *Nature (London)* **393**, 235.
- Krause, F., and K.-H. Rädler, 1980, *Mean-field Magnetohydrodynamics and Dynamo Theory* (Akademie, Berlin).
- Kuang, W., and J. Bloxham, 1997, *Nature (London)* **389**, 371.
- Kumar, S., and P. H. Roberts, 1975, *Proc. R. Soc. London, Ser. A* **344**, 235.
- Larmor, J., 1919, *Br. Assoc. Adv. Sci.* 159–160.
- Lehnert, B., 1958, *Ark. Fys.* **13**, 10, 109.
- Léorat, J., P. Lallemand, J. L. Guermond, and F. Plunian, 2001, in *Dynamo and Dynamics, a Mathematical Challenge*, edited by P. Chossat, D. Armbruster, and I. Oprea (Kluwer, Dordrecht), pp. 25–33.
- Lilley, F. E. M., 1970, *Proc. R. Soc. London, Ser. A* **316**, 153.
- Loves, F. J., and I. Wilkinson, 1963, *Nature (London)* **198**, 1158.
- Loves, F. J., and I. Wilkinson, 1968, *Nature (London)* **219**, 717.
- Malkus, W. V. R., 1994, in *Lectures on Solar and Planetary Dynamos*, edited by M. R. E. Proctor and A. D. Gilbert (Cambridge University, Cambridge, England), pp. 161–179.
- Marié, L., J. Burguete, A. Chiffaudel, F. Daviaud, D. Ericher, C. Gasquet, F. Pétrélis, S. Fauve, M. Bourgoin, M. Moulin, P. Odier, J.-F. Pinton, A. Guigon, J.-B. Luciani, F. Namer, and J. Leorat, 2001, in *Dynamo and Dynamics, a Mathematical Challenge*, edited by P. Chossat, D. Armbruster, and I. Oprea (Kluwer, Dordrecht), pp. 35–50.
- Marié, L., F. Pétrélis, M. Bourgoin, J. Burguete, A. Chiffaudel, F. Daviaud, S. Fauve, P. Odier, and J.-F. Pinton, 2002, *Magnetohydrodynamics* **38**, 163.
- Merrill, R. T., M. W. McElhinny, and Ph. L. McFadden, 1998, *The Magnetic Field of the Earth: Paleomagnetism, the Core, and the Deep Mantle* (Academic, San Diego).
- Merrill, R. T., and P. L. McFadden, 1999, *Rev. Geophys.* **37**, 201.
- Moffatt, H. K., 1978, *Magnetic Field Generation in Electrically Conducting Fluids* (Cambridge University, Cambridge, England).
- Müller, U., and R. Stieglitz, 2000, *Naturwissenschaften* **87**, 381.
- Nakajima, T., and M. Kono, 1991, *Geophys. Astrophys. Fluid Dyn.* **60**, 177.
- Needham, J., 1962, *Science and Civilisation in China* (Cambridge University, Cambridge, England), Vol. 4, Pt. 1.
- Ness, N. F., K. W. Behannon, R. P. Lepping, and Y. C. Whang, 1975, *Nature (London)* **255**, 204.
- O'Connell, R., R. Kendrick, M. Nornberg, E. Spence, A. Bayliss, and C. B. Forest, 2001, in *Dynamo and Dynamics, a Mathematical Challenge*, edited by P. Chossat, D. Armbruster, and I. Oprea (Kluwer, Dordrecht), pp. 59–66.
- Olesen, P., 1996, *Phys. Lett. B* **366**, 117.
- Peffley, N. L., A. B. Cawthorne, and D. P. Lathrop, 2000, *Phys. Rev. E* **61**, 5287.
- Peffley, N. L., A. G. Goumivlevski, A. B. Cawthorne, and D. P. Lathrop, 2000, *Geophys. J. Int.* **141**, 52.
- Pekeris, C. L., Y. Accad, and B. Shkoller, 1973, *Philos. Trans. R. Soc. London, Ser. A* **275**, 425.
- Petrus Peregrinus de Maricourt, 1995, *Opera* (Scuola Normale Superiore, Pisa).
- Pierson, E. S., 1975, *Nucl. Sci. Eng.* **57**, 155.
- Plunian, F., P. Marty, and A. Alemany, 1999, *J. Fluid Mech.* **382**, 137.
- Ponomarenko, Yu. B., 1973, *J. Appl. Mech. Tech. Phys.* **14**, 775.
- Rädler, K.-H., A. Apel, E. Apstein, and M. Rheinhardt, 1996, *Astrophysical Institute, Potsdam, Report*.
- Rädler, K.-H., E. Apstein, M. Rheinhardt, and M. Schüler, 1998, *Stud. Geophys. Geod.* **42**, 1.
- Rädler, K.-H., M. Rheinhardt, E. Apstein, and H. Fuchs, 2002a, *Magnetohydrodynamics* **38**, 41.
- Rädler, K.-H., M. Rheinhardt, E. Apstein, and H. Fuchs, 2002b, *Magnetohydrodynamics* **38**, 73.
- Reighard, A. B., and M. R. Brown, 2001, *Phys. Rev. Lett.* **86**, 2794.
- Roberts, G. O., 1972, *Philos. Trans. R. Soc. London, Ser. A* **271**, 411.
- Roberts, P. H., 1994, in *Lectures on Solar and Planetary Dynamos*, edited by M. R. E. Proctor and A. D. Gilbert (Cambridge University, Cambridge, England), pp. 1–58.
- Roberts, P. H., and G. A. Glatzmaier, 2000, *Rev. Mod. Phys.* **72**, 1081.
- Roberts, P. H., and T. H. Jensen, 1992, *Phys. Fluids B* **7**, 2657.
- Roberts, P. H., and A. M. Soward, 1992, *Annu. Rev. Fluid Mech.* **24**, 459.
- Rüdiger, G., and R. Arlt, 1999, in *Advances in Nonlinear Dynamics, The Fluid Mechanics of Astrophysics and Geophysics* Vol. 8, edited by A. Ferriz-Mas and M. M. Jiménez (Gordon and Breach, London).
- Rüdiger, G., and Y. Zhang, 2001, *Astron. Astrophys.* **378**, 302.
- Ruzmaikin, A., D. Sokoloff, and A. Shukurov, 1988, *J. Fluid Mech.* **197**, 39.
- Shew, W. L., D. R. Sisan, and D. P. Lathrop, 2001, in *Dynamo and Dynamics, a Mathematical Challenge*, edited by P. Chossat, D. Armbruster, and I. Oprea (Kluwer, Dordrecht), pp. 83–92.
- Siemens, C. W., 1867, *Proc. R. Soc. London* **15**, 367.
- Simonyi, K., 1990, *Kulturgeschichte der Physik* (Urania, Leipzig), p. 343.
- Southwood, D. J., 1997, *Planet. Space Sci.* **45**, 113.

- Steenbeck, M., I. M. Kirko, A. Gailitis, A. P. Klawina, F. Krause, I. J. Laumanis, and O. A. Lielausis, 1967, *Monatsber. Dtsch. Akad. Wiss. Berlin* **9**, 714.
- Steenbeck, M., F. Krause, and K.-H. Rädler, 1966, *Z. Naturforsch. A* **21a**, 369.
- Stefani, F., G. Gerbeth, and A. Gailitis, 1999, in *Transfer Phenomena in Magneto hydrodynamic and Electroconducting Flows*, edited by A. Alemany, Ph. Marty, and J. P. Thibault (Kluwer, Dordrecht), pp. 31–44.
- Stefani, F., G. Gerbeth, and K.-H. Rädler, 2000, *Astron. Nachr.* **321**, 65.
- Stieglitz, R., and U. Müller, 1996 (Forschungszentrum Karlsruhe), Report FZKA 5716.
- Stieglitz, R., and U. Müller, 2001, *Phys. Fluids* **13**, 561.
- Tilgner, A., 1997a, *Acta Astron. et Geophys. Univ. Comeniana* **XIX**, 51.
- Tilgner, A., 1997b, *Phys. Lett. A* **226**, 75.
- Tilgner, A., 2000, *Phys. Earth Planet. Inter.* **117**, 171.
- Tilgner, A., 2002, unpublished.
- Tilgner, A., and F. H. Busse, 2001, in *Dynamo and Dynamics, a Mathematical Challenge*, edited by P. Chossat, D. Armbruster, and I. Oprea (Kluwer, Dordrecht), pp. 109–116.
- Wheatstone, C., 1867, *Proc. R. Soc. London* **15**, 369.
- Wilkinson, I., 1984, *Geophys. Surv.* **7**, 107.
- Zandbergen, P. J. and D. Dijkstra, 1987, *Annu. Rev. Fluid Mech.* **19**, 465.
- Zhang, K., and G. Schubert, 2000, *Annu. Rev. Fluid Mech.* **32**, 409.